



## Wind Tunnel Testing Of Tapered Wing For Flutter Analysis With NACA 64-210 At The Tip And NACA 64-215 At The Root

<sup>1</sup> Dr. Nataraj Kuntoji, <sup>2</sup> Dr. Vinay V Kuppast

<sup>1</sup>Sr.Gr.Lecturer, <sup>2</sup>Professor

<sup>1</sup>Department of Mechanical Engineering, Government Polytechnic Basavan Bagewadi, Vijayapura, Karnataka, India

<sup>2</sup> Department of Mechanical Engineering, Basaveshwar Engineering College, (Affl. to Visvesvaraya Technological University, Belgaum) Bagalkot, India

**Abstract:** The primary investigation in the aerodynamics is to study how the objects fly in the air. Study of flutter analysis is to be considered in the aircraft wing design. In this work the comprehensive study of tapered 3D asymmetrical airfoil wing is focused. There have been the studies which proved to be acceptable by adopting simulation tools and then by experimental validation. In the present study the CAE approach is used to model the aircraft wing according to NACA standards and this model is used for Computational Fluid Dynamics (CFD) analysis. The tapered wing is modeled in CATIA V5 considering NACA 64-210 at the tip and NACA 64-215 at the root. CFD is carried out using ANSYS Fluent R20. The Reynolds number of  $3.5 \times 10^6$  (30m/s) is considered, which resembles the subsonic speed. The wing considered for the present study is analyzed for the flutter. The wind tunnel experiment is carried out to determine the frequency and amplitude at different angles of attack (AOA) ranging from  $0^\circ$  to  $20^\circ$ . This indicates that the flutter boundary occurs at the lower frequency range for the tapered wing between 0 Hz to 50 Hz. The occurrence of maximum amplitude during lower frequency range certainly not desirable characteristic for the aircraft wing design.

**Index Terms** - CFD Analysis, NACA 64-215, NACA 64-210, Flutter Analysis, Tapered Wing.

### I. INTRODUCTION

Airfoil sections have been developed during 1800s. Predominantly the study of airfoil sections depends on boundary layer theory developed by Ludwig Prandtl. In his theory, fluid flowing over an object is divided and flows as two regions i. laminar region i.e. outside flow region and ii. region near to the object. This in turn causes the air to flow at different velocities at the lower and upper surface of the object that comes in the flow of air [1]. Figure 1 shows the transverse cross-section of the aircraft wing is called airfoil which obeys the boundary layer theory [2, 3].

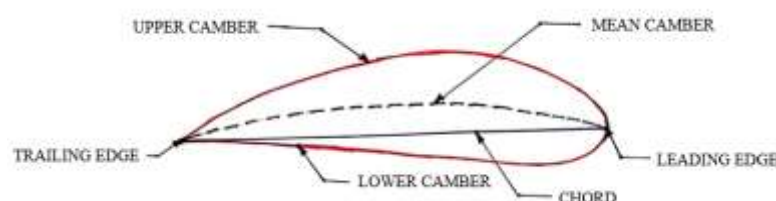


Figure 1 Cross-section of the Aircraft Wing

The airfoil function is to sling the entire weight of the aircraft in the air. The airfoil is designed in such a way that when it moves with specified speed produces an aerodynamic force which is useful to lift the aircraft in the air due to the velocity between the airfoil and the air called relative velocity. The lift is the force produced due to the difference in the pressure on the upper and lower surface of the wing or airfoil. Drag force is shear force (parallel) which is acting opposite to the aircraft forward motion direction resulting in the more utilization of energy to overcome the shear force or drag force [4]. Vinayak Chumber et al, carried out study on various National Advisory Committee for Aeronautics (NACA) profiles to find the lift and drag coefficients and concluded at the end that high coefficient of lift is generated for higher angle of attack and simultaneously it experiences the higher drag force. [5]. Chandrakant Sagat et al. carried out both CFD and Experimental analysis at subsonic speeds and he was concluded that for a particular angle of attack that to at  $12^\circ$  the lift coefficient starts decreasing with small amount of increase in the drag coefficient[6]. Jon Leary carried out CFD analysis on wind turbine blades to see the behavior of lift and drag coefficient [7]. Bhosle et al. plotted the graph of angle of attack Vs coefficient of lift and angle of attack Vs coefficient of drag, the same he has repeated for various angle of attack [8]. Ankan Dash, concluded in his research that lift coefficient increases with decrease in the drag coefficient up to critical angle of attack, after certain angle of attack it reverses [9]. Eleni et al. considered NACA 0012 for lift and drag coefficient variation study at Reynolds number  $3.0 \times 10^6$  for dissimilar viscous turbulence models namely realizable k- $\epsilon$ , Spalart-Allmaras, and SST models and arrived that experimental results were better matching the SST model results [10].

## II. CONSTRUCTION OF TAPERED WING PROFILE

The aircraft wing is modeled in CATIA V5 considering NACA 4412 airfoil with predefined coordinates [11]. S. Senthilkumar et al modeled tapered aircraft wing in CATIA V5 with NACA 65-210 airfoil coordinates [12]. Guguloth Kavya and B. C. Raghukumar Reddy were modeled aircraft wing in ProE with spars and ribs [13], Kakumani Sureka and R. Satya Meher have modeled aircraft wing in CATIA V5 R20 CAD software using NACA 64-215 airfoil coordinates [14]. From these literature surveys it is concluded that CATIA V5 is the best CAD tool to model the taper wing. Airfoil NACA 64-210 at the tip and NACA 64-215 at the root are used to build the tapered wing and the basic size requirements are considered from [15] and the coordinates to generate the airfoil are taken from [16]. Initially coordinate points are generated as shown in the Figure 2; spine is created by joining the points as shown in the Figure 3.



Figure 2 Generation of Coordinates at root and tip with predefined macros in CATIA V5.

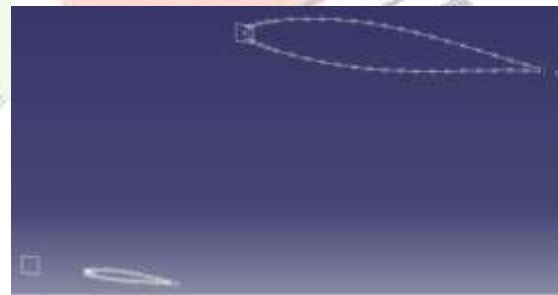


Figure 3 Airfoil shape creation using spline in CATIA V5

Wing surface is created by joining the two airfoil's one at the root and another at the tip as shown in the Figure 4.

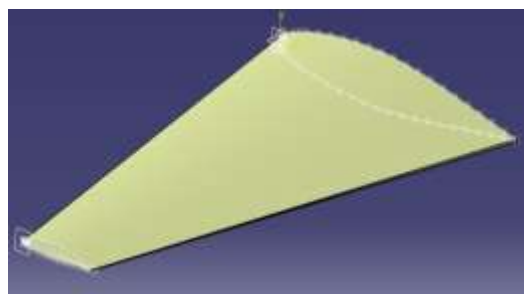


Figure 4 Wing surface connecting root and tip sections

### III. PROTOTYPE BY 3D PRINTING

Fused Deposition Modeling is a process that employs dried thermoplastic filament that is then shoved out layer upon layer to build a 3D object [17]. FDM technology was introduced by Scott Crump in the early 1990s by Stratasys INC, USA. The 3D printers used for FDM include a support base that is related to some degree of freedom and is arranged in such a way that it moves vertically. Aboard the bottom plate is an associate extruder that links the filament and is responsible for heating the filament up to its freezing point and then extruding it layer by layer with the help of a nozzle to construct the desired item. The extruder has enough power to move in all three directions (x, y, and z). The name "fused deposition modeling" comes from the fact that the neighboring layers are merged to one another when deposition is finished by the extruder, and so the 3D printer is responsible for modeling the object. Figure 5 shows the setup of FDM method. By using FDM 3D printing method two wings have been manufactured one without washout (twisted) as shown in the Figure 6.



Figure 5 Fused Deposition 3D printing setup



Figure 6 3D Printed wing without washout

### IV. WIND TUNNEL TESTING

The wind tunnel considered is subsonic wind tunnel where in it operates the air speed up to 80m/s as shown in Figure 7.



Figure 7 Subsonic wind tunnel Velocity up to 80 m/s

The fabricated model was setup for conducting the experiment in the wind tunnel. The wind tunnel specifications are given in Table 1.

Table 1. Specification of Wind Tunnel Used

Type	Low speed subsonic wind tunnel
Test Section	600x600 mm
Length	2m
Maximum speed	83 m/s
Maximum RPM	1300 RPM
Contraction Ratio	9:1

The optimized wing models without washout and with washout are tested for vibration characteristics. This is carried out by flutter analysis of the wing. The plots of frequency Vs Amplitude and time Vs displacement depict of flutter of a wing showing the amplitude of wing oscillation changes as a function of the excitation frequency.

This graph can help engineers and researchers understand the behavior of the wing's aero elastic system and identify the flutter boundary, which is the region where the wing is prone to flutter instability.

The position of 3-axes ADXL 335 accelerometer sensors fixed on the wing for the data logging is shown in the Figure 8, and the axes representation is shown in the Table 2

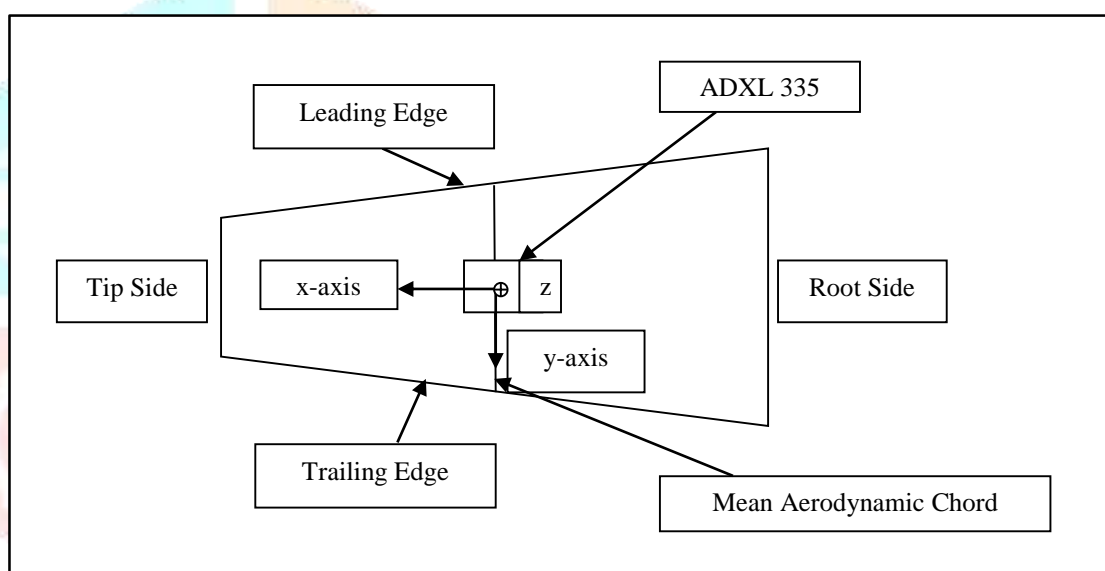


Table 2 Axis representation of the ADXL 335 Sensor placed on the wing

Axes of Sensor	Representation
X - Axis	Along the span of the wing.
Y - Axis	Along Lateral direction of the wing.
Z - Axis	Perpendicular to the span and along the direction of lift of the wing.

The Z- axis data of the sensor is considered for the flutter of the wing since the amplitude of vibration along z-axis is more significant parameter than the other two axes. However, for the understanding of overall vibration, the wing flutter along X and Y axes are also observed.

In the Wing Flutter Plots, the horizontal axis represents the excitation frequency of the wing's oscillations. This can be expressed in terms of frequency (Hertz). The vertical axis represents the amplitude of the wing's oscillations. This is typically shown as the maximum displacement or deflection of the wing from its equilibrium position.



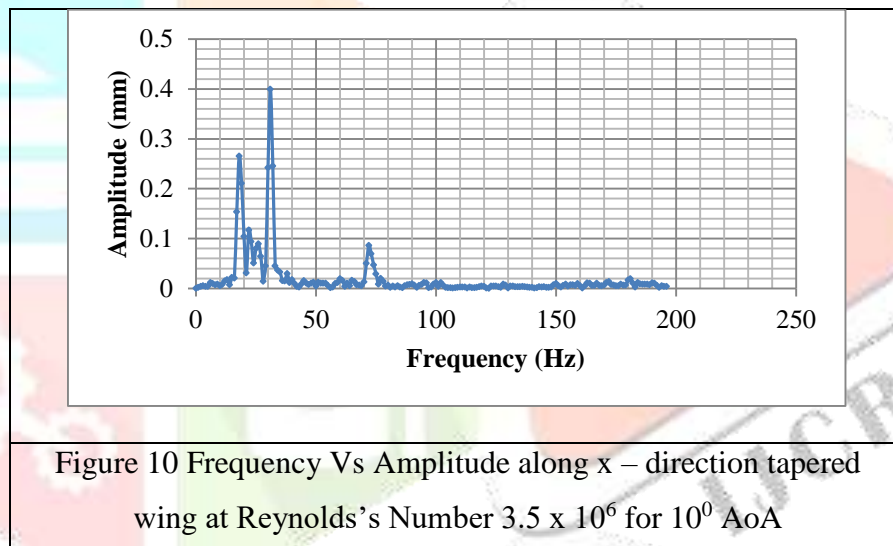
In a flutter region at a certain frequency, the amplitude suddenly increases significantly. This is the flutter boundary. The amplitude becomes large and can lead to unstable oscillations if not addressed. Engineers aim to design aircraft to operate below this boundary. For flutter analysis the wing is placed on the wind tunnel in the air flow stream as shown in Figure 9.



Figure 9 Wing is placed on the wind tunnel

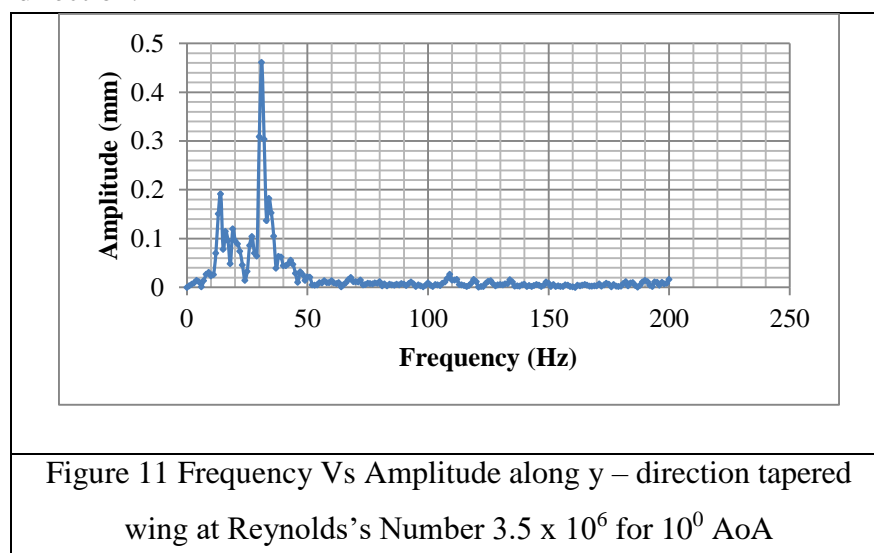
## V. RESULTS AND DISCUSSIONS

- Flutter plot for the tapered wing at Reynolds's Number  $3.5 \times 10^6$  for  $10^\circ$  AoA is shown in the Figure 10 in the x – direction.



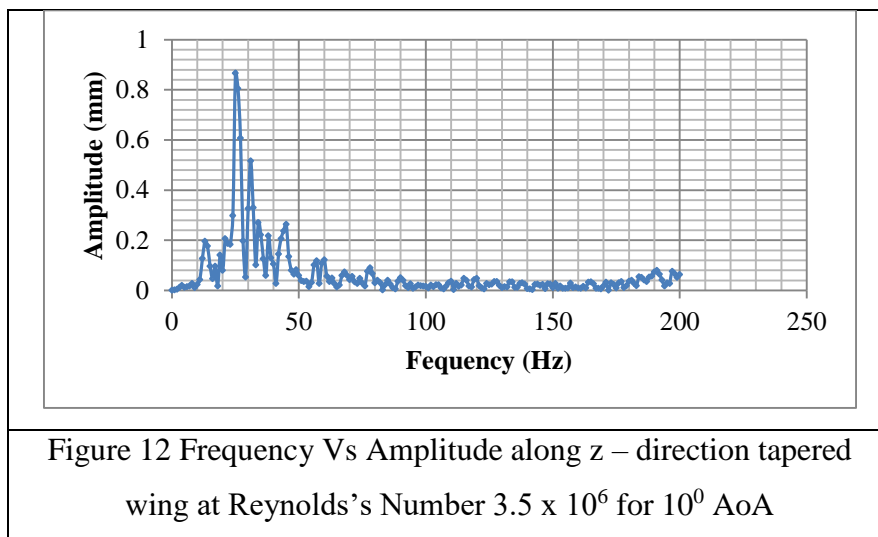
From Figure 10 the maximum amplitude of 0.399 mm is observed between the frequency ranges of 0 Hz to 50 Hz.

- Flutter plot for the tapered wing at Reynolds's Number  $3.5 \times 10^6$  for  $10^\circ$  AoA is shown in the Figure 11 in the y – direction.



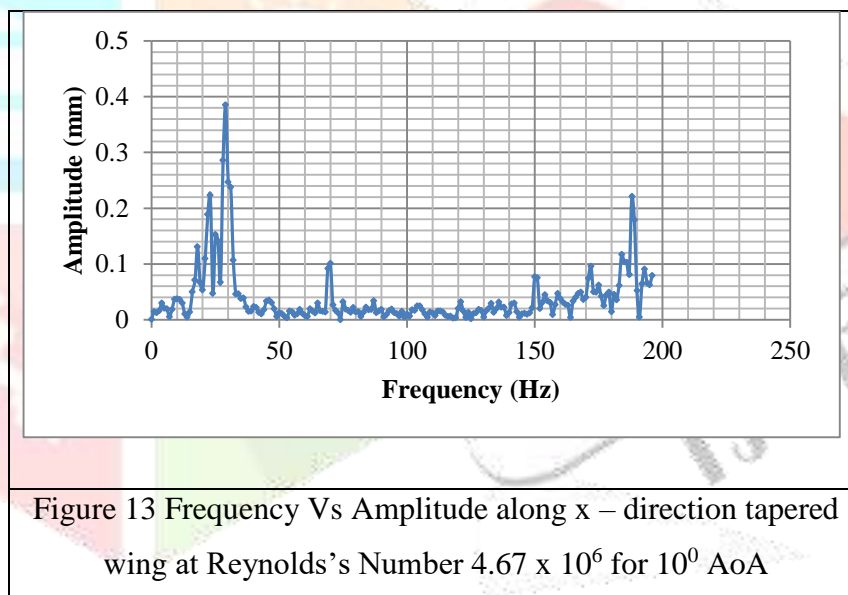
From Figure 11 the maximum amplitude of 0.461 mm is observed between the frequency ranges of 0 Hz to 50 Hz.

- Flutter plot for the tapered wing at Reynolds's Number  $3.5 \times 10^6$  for  $10^0$  AoA is shown in the Figure 12 in the z – direction.



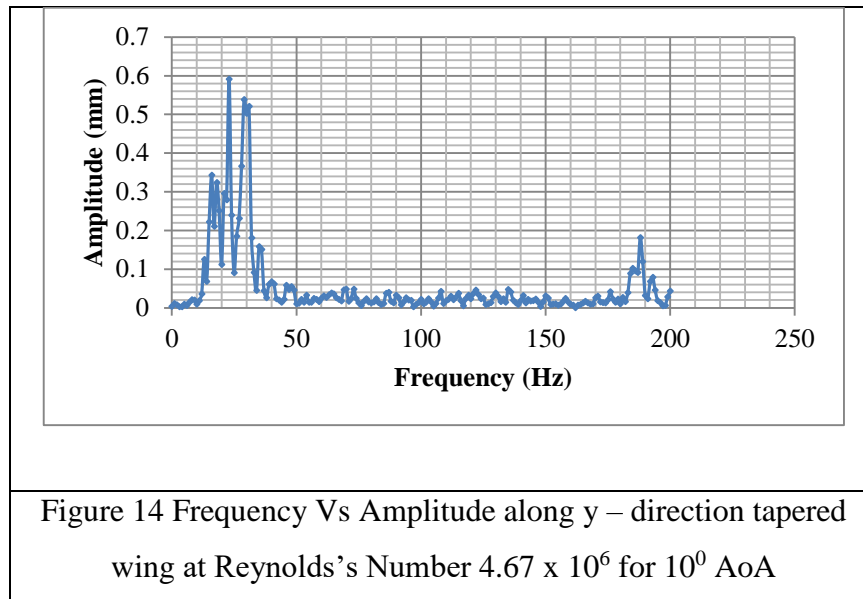
From Figure 12 the maximum amplitude of 0.866 mm is observed between the frequency ranges of 0 Hz to 50 Hz.

- Flutter plot for the tapered wing at Reynolds's Number  $4.67 \times 10^6$  for  $10^0$  AoA is shown in the Figure 13 in the x – direction.



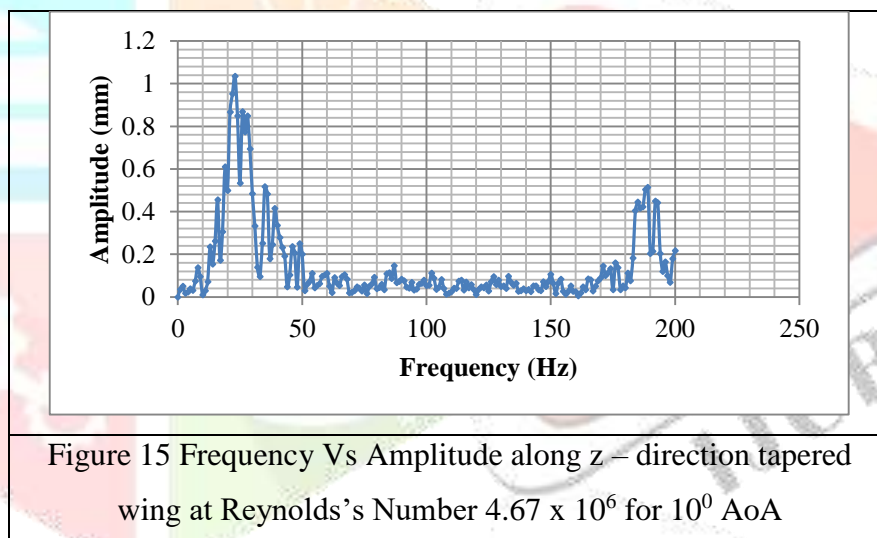
From Figure 13 the maximum amplitude of 0.385 mm is observed between the frequency ranges of 0 Hz to 50 Hz.

5. Flutter plot for the tapered wing at Reynolds's Number  $4.67 \times 10^6$  for  $10^\circ$  AoA is shown in the Figure 14 in the y – direction.



From Figure 14 the maximum amplitude of 0.591 mm is observed between the frequency ranges of 0 Hz to 50 Hz.

6. Flutter plot for the tapered wing at Reynolds's Number  $4.67 \times 10^6$  for  $10^\circ$  AoA is shown in the Figure 15 in the z – direction.



From Figure 15 the maximum amplitude of 1.034 mm is observed between the frequency ranges of 0 Hz to 50 Hz.

This indicates that the flutter boundary occurs at the lower frequency range for the wing without washout between 0 Hz to 50 Hz. The occurrence of maximum amplitude during lower frequency range certainly not desirable characteristic for the aircraft wing design.

## VI. CONCLUSIONS

Literature related to aerodynamic characteristic analysis using CFD involves 2D airfoil only. In this research work 3D tapered asymmetrical wing is considered. Tapered asymmetrical wing is modeled in CATIA V5 R19 using NACA 64-210 at the tip and NACA 64-215 at the root. Wind tunnel testing is carried out for flutter analysis. Reynolds number  $3.5 \times 10^6$  (30m/s) is considered. This indicates that the flutter boundary occurs at the lower frequency range for the tapered wing between 0 Hz to 50 Hz. The occurrence of maximum amplitude during lower frequency range certainly not desirable characteristic for the aircraft wing design. To improve the range of the frequency with low amplitude is achieved with twist in the wing.

## VII. REFERENCES

- [1] Yunus A. Cengel, John M. Cimbala, Textbook on Fluid Mechanics, Tata McGraw Hill Publication, 2014.
- [2] Triet MM, Viet NN, Thang PM. Aerodynamic analysis of aircraft wing. VNU J. Sci. Math. – Phys. 2015;31(2):68–75.
- [3] Zhang Y, Fang X, Chen H, Fu S, Duan Z, Zhang Y. Supercritical natural laminar flow airfoil optimization for regional aircraft wing design. Aerospace. Sci. Technol. 2015; 43:152–164.
- [4] Kevadiya M. CFD analysis of pressure coefficient for NACA 4412. International Journal of Engineering Trends and Technology. 2013; 4:5.
- [5] Vinayak Chumber, T. Rushikesh, Sagar Umatar, Shirish M. Kerur, CFD analysis of airfoil section, IRJET 5 (18) (2018) 349–353.
- [6] Chandra Kant Sagat, Experimental and CFD analysis of Airfoil at low Reynolds number, Int. J. Mech. Eng. Robot. Res. 1 (3) (2012) 227–283.
- [7] Jon Leary, Computational Fluid dynamics analysis of a low-cost wind turbine, EPSRC (2010).
- [8] Bhosle O, Varpe R, Pula M. Radio controlled airplane. International Journal for Scientific Research & Development. 2013; 3:2.
- [9] Ankan Dash, CFD analysis of wind turbine airfoil at various angles of attack, J. Mech. Civ. Eng. 13 (2016) 18–24.
- [10] Eleni DC, Athanasios TI, Dionissios MP. Evaluation of the turbulence models for the simulation of the flow over a National Advisory Committee for Aeronautics (NACA) 0012 Airfoil. Journal of Mechanical Engineering Research. 2012;4(3):100-111.
- [11] Sudhir Reddy Konayapalli and Y Sujatha “Design and Analysis of Aircraft Wing” International Journal and Magazine of Engineering, Technology, Management and Research. Volume No: 2 (2015), Issue No: 9 (September).
- [12] S. Senthilkumar, A. Velayudham, and P. Maniarasan “Dynamic Structural Response Of An Aircraft Wing Using Ansys” International Journal of Engineering Research & Technology (IJERT), Vol. 2 Issue 6, June – 2013.
- [13] Guguloth Kavya and B.C Raghukumar Reddy “Design and Finite Element Analysis of Aircraft Wing using Ribs and Spars” International Journal and Magazine of Engineering, Technology, Management and Research. Volume No: 2 (2015), Issue No: 11 (November).
- [14] Kakumani Sureka and R Satya Meher “Modeling and Structural Analysis on A300 Flight Wing by using ANSYS” International Journal of Mechanical Engineering and Robotics Research Vol. 4, No. 2, April 2015.
- [15] T.S. Vinoth Kumar, A. Waseem Basha, M. Pavithra, V. Srilekha “Static and Dynamic Analysis of a Typical Aircraft Wing Structure using MSC Nastran” International Journal of Research in Aeronautical and Mechanical Engineering, Volume: 3 Issue 8, August 2015.
- [16] <http://www.pdas.com/sections6a.htm>
- [17] A. Chadha, M. Ul Haq, A. Raina, R. Singh, N. Penumarti, M. Bishnoi, “Effect of fused deposition modelling process parameters on mechanical properties of 3D printed parts”, World J. Eng. 16 (4) (2019) 550–559